

1 **High-latitude stratospheric aerosol geoengineering can**  
2 **be more effective if injection is limited to spring**

3 **Walker Lee<sup>1</sup>, Douglas G. MacMartin<sup>1</sup>, Daniele Vioni<sup>1</sup>, Ben Kravitz<sup>2,3</sup>**

4 <sup>1</sup>Sibley School for Mechanical and Aerospace Engineering, Cornell University, Ithaca, NY, USA

5 <sup>2</sup>Department of Earth and Atmospheric Science, Indiana University, Bloomington, IN, USA

6 <sup>3</sup>Atmospheric Sciences and Global Change Division, Pacific Northwest National Laboratory, Richland,  
7 WA, USA

8 **Key Points:**

- 9 • Stratospheric aerosol geoengineering in the Arctic could reduce some impacts of  
10 climate change  
11 • Aerosols present in summer reflect more light and therefore affect the climate more  
12 efficiently  
13 • Our study shows that spring injections restore twice the summer sea ice as year  
14 round injections

---

Corresponding author: Walker Lee, [w1644@cornell.edu](mailto:w1644@cornell.edu)

## Abstract

Stratospheric aerosol geoengineering focused on the Arctic could substantially reduce local and worldwide impacts of anthropogenic global warming. Because the Arctic receives little sunlight during the winter, stratospheric aerosols present in the winter at high latitudes have little impact on the climate, whereas stratospheric aerosols present during the summer achieve larger changes in radiative forcing. Injecting SO<sub>2</sub> in the spring leads to peak aerosol optical depth (AOD) in the summer. We demonstrate that spring injection produces approximately twice as much summer AOD as year-round injection and restores approximately twice as much September sea ice, resulting in less increase in stratospheric sulfur burden, stratospheric heating, and stratospheric ozone depletion per unit of sea ice restored. We also find that differences in AOD between different seasonal injection strategies are small compared to the difference between annual and spring injection.

## Plain Language Summary

Scattering small particles called aerosols into the sky - “geoengineering” - could reflect a small amount of sunlight in order to combat global warming. Doing this near the Arctic could help stop sea ice from melting, which would help preserve the Arctic climate. Our study shows that, for Arctic geoengineering, scattering particles in the spring is most efficient because the particles will be present throughout the summer, and the Arctic receives the most sunlight in the summer. Therefore, spring Arctic geoengineering could accomplish the same goals as year-round Arctic geoengineering, but with fewer particles and thus fewer negative side-effects.

## 1 Introduction

Arctic sea ice reflects solar radiation, regulates the exchange of energy and moisture between the ocean and the atmosphere, affects the thermohaline circulation and biogeochemistry of the Arctic, and serves as a habitat for ice-dwelling fauna (Meredith et al., 2019; D. Perovich et al., 2020; Barber et al., 2017). Since the beginning of the 21<sup>st</sup> century, the Arctic has warmed more than twice as fast as the global average (Meredith et al., 2019; Ballinger et al., 2020), leading to decreases in the surface area and thickness of Arctic sea ice. The decline is largest during the annual minimum in September, where sea ice extent has been shrinking by an average of 83,000 km<sup>2</sup> per year, or 13% per decade (Meredith et al., 2019; D. Perovich et al., 2020; J. Stroeve & Notz, 2018). Increases in greenhouse gas (GHG) concentrations are the primary external driver for loss of sea ice in the Arctic (Kay et al., 2011; Notz & Marotzke, 2012; Fyfe et al., 2013), and this impact is likely underestimated by climate models (Notz & Stroeve, 2016). While climate models disagree on the exact rate of Arctic sea ice loss, they predict summer ice extent will drop below one million square kilometers by 2039-2045 regardless of emissions scenario (Snape & Forster, 2014) and that summer sea ice will eventually be lost in all shelf seas in all scenarios (Årthun et al., 2021). Projections of current trends suggest Arctic sea ice extent will wane more quickly than climate models predict, and that the Arctic may lose all of its September sea ice by 2035-2040 (Peng et al., 2018; J. Stroeve & Notz, 2018; Barber et al., 2017). Additionally, as the summer ice shelves retreat, a greater fraction of the Arctic is covered in young seasonal sea ice during the winter, which is thinner than multi-year sea ice and therefore more fragile and less reflective (D. Perovich et al., 2020; Barber et al., 2017; J. Stroeve & Notz, 2018; Meredith et al., 2019). This ice-albedo feedback further drives polar warming and Arctic amplification (Haine & Martin, 2017; Pithan & Mauritsen, 2014; D. K. Perovich & Polashenski, 2012; J. C. Stroeve et al., 2012); the ice-albedo feedback increased radiative heating in the Arctic Ocean by 6.4 Wm<sup>-2</sup> between 1979 and 2014 (Pistone et al., 2014), resulting in 3-4 K of additional warming in the Arctic (Pithan & Mauritsen, 2014).

65 Mitigation of future CO<sub>2</sub> emissions alone may not be sufficient to prevent future  
66 climate impacts due to uncertainty in both the rate of future mitigation and in the cli-  
67 mate response (Rogelj et al., 2016), and stratospheric aerosol injection (SAI) has been  
68 suggested as a possible temporary supplement to mitigation and carbon dioxide removal.  
69 There have been a number of simulations of “global” SAI strategies with the aim of main-  
70 taining a desired global mean temperature or other climate goals: the Geoengineering  
71 Large Ensemble (GLENS) study injected SO<sub>2</sub> at 30°N, 15°N, 15°S, and 30°S to try and  
72 stabilize global mean temperature alongside the interhemispheric and equator-to-pole  
73 temperature gradients (Kravitz et al., 2017; Tilmes et al., 2018), and the G3 and G4 ex-  
74 periments of the Geoengineering Model Intercomparison Project (GeoMIP) injected SO<sub>2</sub>  
75 above the equator to offset increases in radiative forcing and global mean temperature  
76 (Kravitz et al., 2011). Several studies have evaluated the Arctic impacts of these “global”  
77 approaches, finding that low- or mid-latitude injections of SO<sub>2</sub> could reduce global-warming-  
78 induced losses of sea ice and permafrost (Jiang et al., 2019; Lee et al., 2020; Moore et  
79 al., 2019; Chen et al., 2020). However, high-latitude SAI intended specifically to preserve  
80 the Arctic has been hypothesized to provide greater Arctic cooling per unit of injection  
81 than low-latitude SAI with smaller effects at low latitudes; for example, high-latitude  
82 injections have been shown to have smaller impacts on tropical precipitation than equa-  
83 torial injections (Sun et al., 2020). Simulations of localized solar reduction northwards  
84 of 50, 60, and/or 70°N (or similar) have been shown to slow or reverse the loss of sea ice  
85 to varying extents (Caldeira & Wood, 2008; MacCracken et al., 2013; Tilmes et al., 2014;  
86 Kravitz et al., 2016). However, solar reduction is at best a limited proxy for SAI because  
87 it fails to account for stratospheric heating, changes to stratospheric ozone concentra-  
88 tions, changes to the stratospheric circulation, and perhaps most important of all, the  
89 actual spatial and seasonal distributions of AOD, which are driven by stratospheric trans-  
90 port (Visioni, MacMartin, & Kravitz, 2020). There have been a few studies of Arctic-  
91 focused SAI: Robock et al. (2008) injected 3 Mt/yr of SO<sub>2</sub> at 68°N, which restored SSI  
92 comparably to 5 Mt per year injected at the equator; Jackson et al. (2015) successfully  
93 managed the restoration and stabilization of SSI through injections at 78.55°N; and Sun  
94 et al. (2020) showed that aerosols present at high-latitudes injections have smaller im-  
95 pacts on tropical precipitation than equatorial injections.

96 There is substantial evidence that high-latitude SAI could, to some degree, coun-  
97 teract Arctic warming and consequent impacts on the Arctic more efficiently than low-  
98 latitude injection. However, to date, most simulated Arctic SAI strategies have been ad  
99 hoc; Jackson et al. (2015) and Lee et al. (2020) are the only strategies which have ac-  
100 tively managed injection rates to maintain a desired SSI concentration, and Jackson et  
101 al. (2015) is the only strategy which has done so by injecting at a high latitude. Little  
102 effort has been undertaken to design an Arctic-focused SAI strategy: what combination  
103 of latitude, altitude, quantity, or timing of the injection will best preserve Arctic climate?  
104 Of these, time of year of injection is likely critical. Visioni, MacMartin, Kravitz, Richter,  
105 et al. (2020) found that injection in different seasons (at lower latitudes) has different  
106 regional climate outcomes. Moreover, the difference between injecting SO<sub>2</sub> year round,  
107 as has been the case for most simulations of SAI to date, and injecting seasonally, is likely  
108 even more critical for higher-latitude-injection Arctic-focused geoengineering due to both  
109 shorter aerosol lifetime and higher seasonality of insolation. Insolation north of 60°N is  
110 at least 10 times greater in summer than in winter (Peixoto & Oort, 1992); at low lat-  
111 itudes, insolation is comparable year-round, but at high latitudes, there is little to no  
112 sunlight in winter, meaning aerosols injected to reflect sunlight are largely useless. Fur-  
113 thermore, SO<sub>2</sub> injections are oxidized by OH, which forms in the presence of sunlight;  
114 since there is little to no sunlight in winter, SO<sub>2</sub> injected during the winter will oxidize  
115 into aerosols much more slowly, if at all. Finally, while sulfate aerosols present in win-  
116 ter oxidize more slowly and reflect less sunlight, interactions with other components of  
117 the atmosphere would still take place, including the trapping of longwave radiation, strato-  
118 spheric ozone depletion, and sulfur deposition. Therefore, there is little purpose to in-  
119 jecting in winter, and aerosols should be concentrated in the summer for maximum ef-

120     fect. SO<sub>2</sub> injected in the spring will oxidize in time to be present as aerosols through-  
121     out the summer period of peak insolation (our results show an oxidation lifetime of ap-  
122     proximately one month), producing greater effects on the climate than if the same quan-  
123     tity of SO<sub>2</sub> were distributed year-round. This hypothesis is supported by the results of  
124     Dai et al. (2018), who compared June and December injections of SO<sub>2</sub> and H<sub>2</sub>SO<sub>4</sub> at  
125     66.3°N; summer SO<sub>2</sub> injections produced 2-3 times greater maximum changes in radiative  
126     forcing than winter SO<sub>2</sub> injections, and summer H<sub>2</sub>SO<sub>4</sub> injections (which do not need  
127     to oxidize and begin reflecting sunlight immediately) produced 3-5 times greater max-  
128     imum changes in radiative forcing than winter H<sub>2</sub>SO<sub>4</sub> injections. While Jackson et al.  
129     (2015) injected SO<sub>2</sub> seasonally, their primary focus was to determine whether sea ice was  
130     controllable rather than on the climate response, and they evaluated neither the differ-  
131     ences relative to annually-constant injection nor the dependence on injection latitude and  
132     timing.

133     In this study, we directly compare year-round Arctic SAI with spring Arctic SAI  
134     to demonstrate that spring Arctic SAI restores more September sea ice (SSI) per unit  
135     of SO<sub>2</sub> injected; additionally, spring Arctic SAI results in less stratospheric sulfur bur-  
136     den, heating, and ozone depletion per unit of SSI restored. We also explore the design  
137     space of seasonal Arctic SAI by comparing the AOD of several different strategies; we  
138     do this by modifying the latitude, timing, and duration of injection while keeping the  
139     total injection per year constant. In Section 2, we describe our climate model and our  
140     simulations. We present our results in Section 3, and in Section 4 we discuss our results  
141     and their implications on future geoengineering research.

## 142     2 Climate Model and Simulations

143     In this study, we present simulations of six new stratospheric aerosol injection strate-  
144     gies. Each simulation begins in the year 2030 and uses the RCP8.5 warming scenario.  
145     In each case, we inject a total of 12 Tg of SO<sub>2</sub> every year at an altitude of 14.7-14.9 km  
146     at a single prescribed latitude. Simulation specifications are described in Table 1. Our  
147     two primary simulations each run for 10 years and compare a seasonal injection strat-  
148     egy to a year-round strategy, both injecting at 60°N. In addition, we conducted four 5-  
149     year simulations to evaluate the effects of timing or latitude of injection. We choose 60°N  
150     as the injection latitude for our primary simulations because we wish to inject north of  
151     the stratospheric polar vortex that acts as a transport barrier for the aerosols (Visioni,  
152     MacMartin, Kravitz, Lee, et al., 2020), but also as far south as possible so as to max-  
153     imize the surface area covered by the aerosols as they are transported northward; this  
154     choice is also supported by the results of MacCracken et al. (2013) and Tilmes et al. (2014),  
155     in which solar reductions poleward of 60°N or thereabouts gave the largest restoration  
156     of SSI.

157     Our strategies were simulated using the Community Earth System Model version  
158     1 with the Whole Atmosphere Community Climate Model as the atmospheric compo-  
159     nent, denoted CESM1(WACCM), and is fully coupled with the Parallel Ocean Program  
160     (POP2) ocean, Community Land Model (CLM)4.5 land, and the Community Ice CodE  
161     (CICE)4 ice components (“CICE: the Los Alamos Sea Ice Model Documentation and  
162     Software User’s Manual”, 2010; WANG et al., 2020). CICE is one of the most widely used  
163     models to simulate the growth, melting and movement of Arctic sea ice, for operational  
164     forecasts and to understand sea-ice processes, and has been thoroughly validated (Roberts  
165     et al., 2018; DuVivier et al., 2020) both in its stand-alone form and coupled with CESM.  
166     CESM was run at a horizontal resolution of 0.9 degrees latitude by 1.25 degrees longi-  
167     tude, and WACCM uses a 70-layer vertical grid with a maximum altitude of 145 km, ap-  
168     proximately 10-6 hPa. The model used the modal aerosol component MAM3 (Liu et al.,  
169     2012), which uses a three-bin distribution, and is fully coupled to radiation and atmo-  
170     spheric chemistry. The atmospheric model has been validated against observations both  
171     in quiescent conditions and in the aftermath of explosive volcanic eruptions (Mills et al.,

**Table 1.** Parameters for the six simulations presented in this study. All simulations begin in 2030; simulations are named after the time of year in which they inject SO<sub>2</sub> and the latitude at which they inject. All simulations inject 12 Tg SO<sub>2</sub>/year, which is distributed evenly among the months of injection.

Simulation	Length	SO <sub>2</sub> /yr	Inj. Months <sup>a</sup>	SO <sub>2</sub> /month	Inj. Latitude
MAM-60	10 years	12 Tg	MAM	4 Tg	60°N
ANN-60	10 years	12 Tg	all	1 Tg	60°N
MAM-67.5	5 years	12 Tg	MAM	4 Tg	67.5°N
MAM-75	5 years	12 Tg	MAM	4 Tg	75°N
AM-60	5 years	12 Tg	AM	6 Tg	60°N
AMJ-60	5 years	12 Tg	AMJ	4 Tg	60°N

<sup>a</sup>MAM = March, April, and May; AM = April and May; AMJ = April, May, and June.

172 2016, 2017) and is reasonably consistent with observations of, amongst other things, strato-  
 173 spheric ozone evolution and polar stratospheric clouds formation (Tilmes et al., 2018 -  
 174 JGR, not BAMS) and their interaction with surface climate (Harari et al., 2019); it has  
 175 also been used extensively for studying stratospheric aerosol geoengineering (Kravitz et  
 176 al., 2017; Tilmes et al., 2018; Vioni, MacMartin, Kravitz, Richter, et al., 2020; Lee et  
 177 al., 2020).

### 178 3 Results

179 In Figure 1, we present the seasonal cycle of stratospheric aerosol optical depth (AOD)  
 180 for all simulations. AOD for all spring injection cases peaks in the summer months, and  
 181 all spring injections achieve a peak AOD approximately 2.5 times greater than that of  
 182 ANN-60 regardless of the timing or latitude of injection. For all MAM injections, this  
 183 peak occurs in June; for AMJ, the peak occurs in July, and for AM, June and July are  
 184 comparable. For MAM-60, we compute an oxidation timescale of approximately four weeks  
 185 based on the decay rates of stratospheric SO<sub>2</sub>, which is consistent with the peak AOD  
 186 occurring one month after injection stops. All spring injections at 60°N have compara-  
 187 ble annual mean AOD profiles, regardless of injection timing. MAM-67.5 produces more  
 188 AOD than MAM-60 everywhere in the Northern Hemisphere and averages 20% more AOD  
 189 at high latitudes; spring injections at 67.5°N might therefore be even more efficient than  
 190 spring injections at 60°N at restoring SSI, but these differences are small compared to  
 191 the difference between either of them and annually constant injection. Annual mean AOD  
 192 for spring injections is higher than that of year-round injection in all latitudes north of  
 193 the equator, regardless of injection latitude or timing. As could be expected, seasonal  
 194 variations in Arctic AOD are significantly larger for spring injection than for year-round  
 195 injection, but ANN-60 Arctic AOD is still higher in summer than in winter due to lower  
 196 production of OH through photolysis of O<sub>3</sub> in the winter and subsequently reduced ox-  
 197 idation of SO<sub>2</sub>. Even though ANN-60 injects in the autumn and winter, winter AOD for  
 198 ANN-60 in the Arctic is comparable to those of spring injections; in December, January,  
 199 and February, the average AOD north of 60°N for ANN-60 is 0.13, while the other sim-  
 200 ulations range from 0.09 (MAM-60) to 0.14 (MAM-67.5). Lastly, we observe that while  
 201 changes in AOD are largest in the Arctic, they are not confined to the Arctic; AOD pro-  
 202 duced by injections at 60°N extends to the mid-latitudes in all seasons for year-round  
 203 injection and into the tropics in the summer for MAM-60. Additional comparisons to  
 204 the AOD of seasonal injections at 30°N and 45°N can be found in the supplementary  
 205 material.

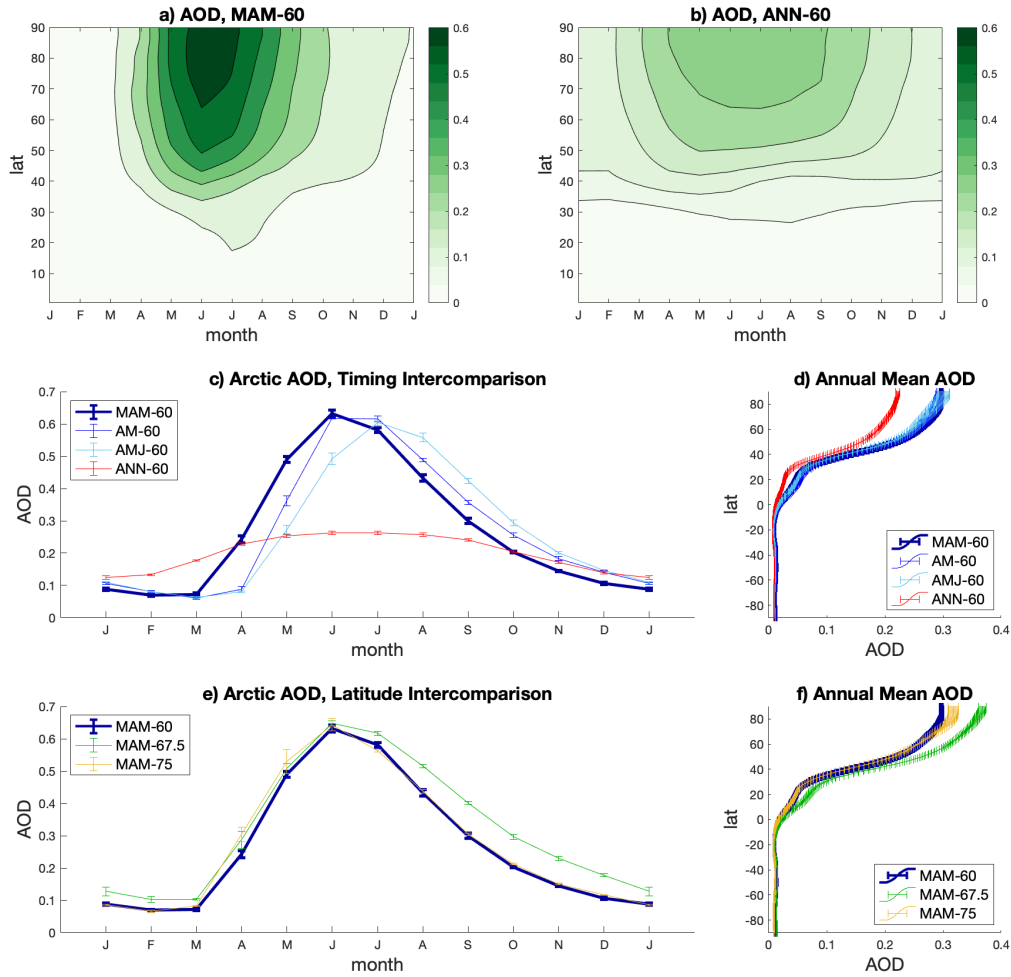


**Figure 1.** AOD for all simulations. Figures 1a and 1b (top row) plot the seasonal cycles of AOD for MAM-60 (left) and ANN-60 (right) as a function of latitude. Figures 1c and 1d (middle row) compare different injection timings, and Figures 1e and 1f (bottom row) compares different injection latitudes; the left panels plot seasonal cycles of Arctic AOD, and the right panels plot annual mean zonal mean AOD as a function of latitude. MAM-60 and ANN-60 data are averaged over the last 5 years of simulation; data from the other simulations are averaged over the last 3 years as in Visoni, MacMartin, Kravitz, Richter, et al. (2020).

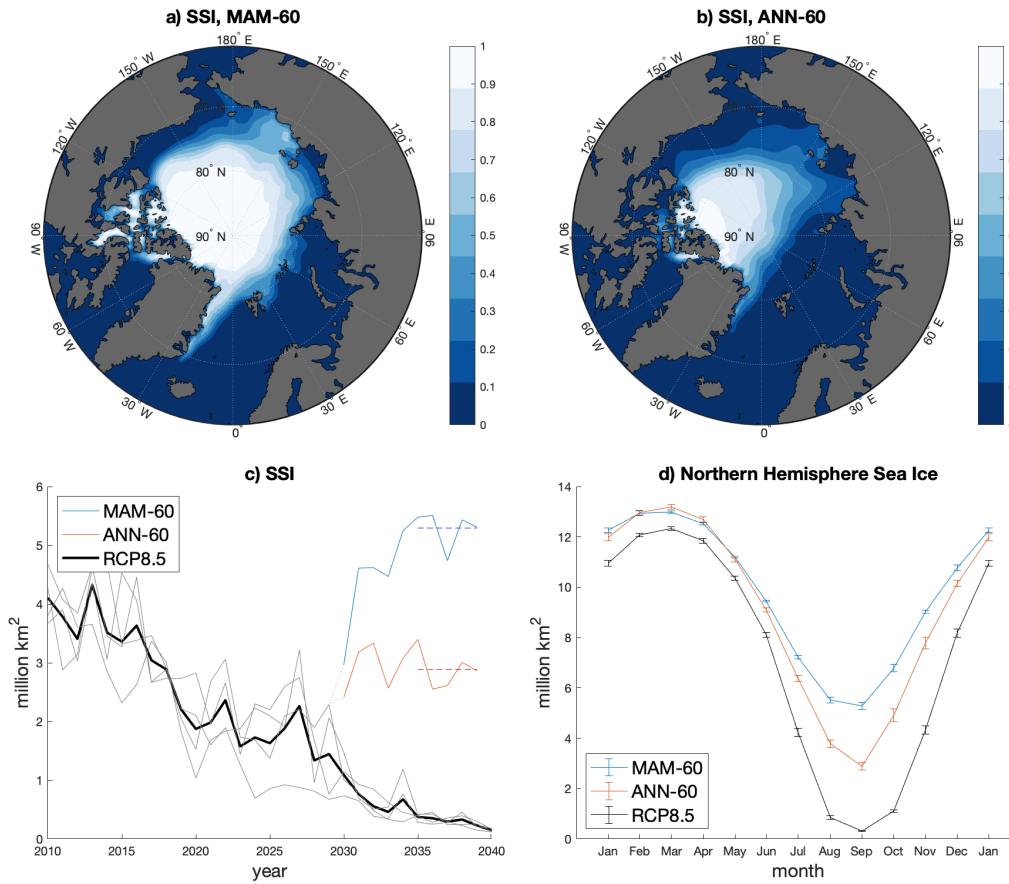


**Figure 2.** Comparison of sea ice between MAM-60 and ANN-60. Figures 2a and 2b (top) show the extent of September Sea Ice (SSI) averaged over the last five years of simulation for each strategy; the color scale denotes the fraction of each grid cell covered in ice. Figure 2c (bottom left) plots SSI over time for both strategies alongside RCP8.5. The thick black line denotes the RCP8.5 ensemble average, while faint black lines denote individual ensemble members; dotted lines connect the blue and red MAM-60 and ANN-60 lines to the ensemble member from which they branched. Horizontal blue and red dashed lines denote the average SSI of MAM-60 and ANN-60, respectively, over the last five years of simulation. Figure 2d (bottom right) plots the seasonal cycle of sea ice for each simulation and for RCP8.5, averaged over the last five years of simulation.

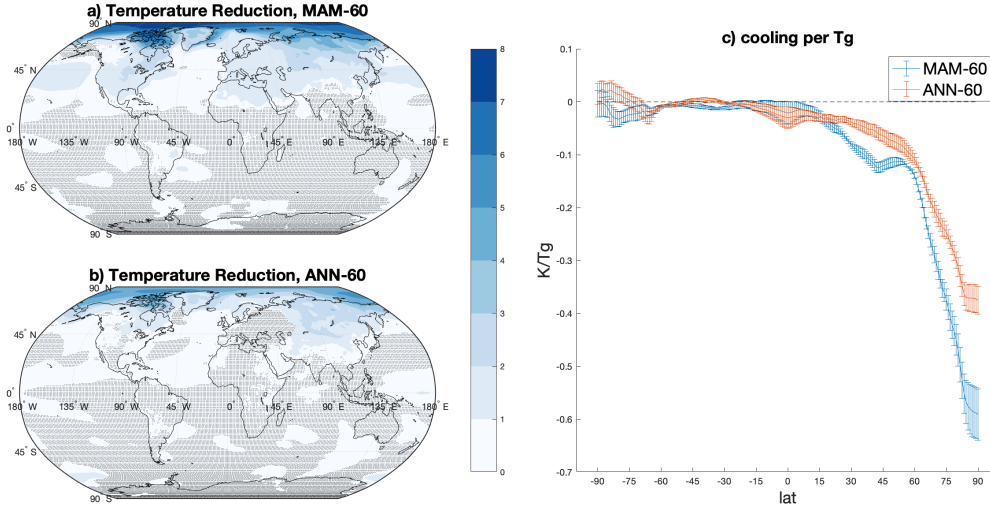


**Figure 3.** Temperature comparison between MAM-60 and ANN-60, averaged over the last five years of simulation, relative to RCP8.5 during the same period (2035-2039). Figures 3a and 3b (left) plots the temperature decrease relative to RCP8.5; gray shading indicates areas where temperature distributions are statistically identical ( $\alpha = 0.5$ ). Figure 3c (right) shows the temperature difference from RCP8.5 as a function of latitude, normalized by injection quantity (12 Tg/yr).

206 Figure 2 shows the behavior of sea ice for MAM-60 and ANN-60, along with RCP8.5  
 207 for comparison. Under RCP8.5, the average SSI in 2035-2039 is  $0.32 \pm 0.02$  million  $\text{km}^2$ ,  
 208 where  $\pm$  value indicates standard error. For ANN-60, this value is  $2.9 \pm 0.2$  million  $\text{km}^2$ ,  
 209 a restoration of 2.6 million  $\text{km}^2$ ; for MAM-60, this value is  $5.3 \pm 0.1$  million  $\text{km}^2$ , a restora-  
 210 tion of 5.0 million  $\text{km}^2$ , approximately twice as much. Sea ice extents for MAM-60 and  
 211 ANN-60 are comparable in the winter. SSI in MAM-60 relative to ANN-60 is both in-  
 212 creased in concentration near the pole as well as extending further from the pole.

213 Figure 3 shows the change in temperature for MAM-60 and ANN-60 relative to RCP8.5  
 214 during the same time period (2035-2039). Temperature changes for both simulations are  
 215 largest in the Arctic but are not confined to the Arctic; Fig. 3a and 3b show statistically  
 216 significant changes for ANN-60 in large parts of Asia and parts of North America and  
 217 for MAM-60 in most of the Northern Hemisphere. The average temperature changes north  
 218 of 60N for MAM-60 and ANN-60 are  $-3.7 \pm 0.2$  K and  $-2.5 \pm 0.2$  K, respectively; the  
 219 global mean temperature changes for MAM-60 and ANN-60 are  $-0.65 \pm 0.06$  K and  $-0.44 \pm$   
 220  $0.06$  K, respectively, a factor of approximately 1.5 for both metrics.

221 In addition to surface cooling, stratospheric sulfate aerosols will warm the strato-  
 222 sphere (Ferraro et al., 2015) and contribute to high-latitude ozone loss (Robrecht et al.,  
 223 2020). In Figure 4, we present annual mean increases in stratospheric sulfate mixing ra-  
 224 tio and its effect on air temperature and ozone concentration for MAM-60 and ANN-  
 225 60; all the changes are normalized by the extent of SSI restored. This way we can eval-  
 226 uate the effects of both strategies based on their efficacy: in this case MAM-60 produces  
 227 smaller changes than ANN-60, and the effects are also more localized. In ANN-60, more  
 228 aerosols are transported equatorward, and aerosols are also present at high latitudes year-  
 229 round. We observe a stratospheric heating peak over the North Pole, as a possible con-  
 230 sequence of both ozone destruction in early spring and the aerosols absorbing more plan-  
 231 etary radiation in the winter months. Additionally, ANN-60 shows some ozone increase

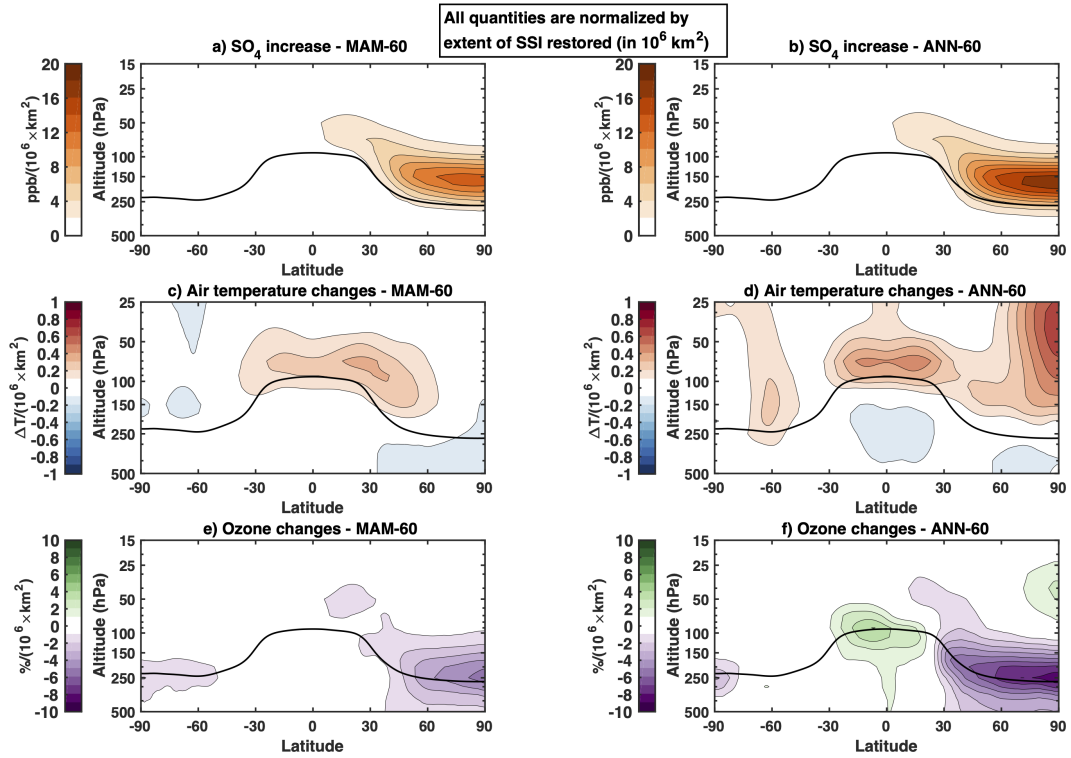


**Figure 4.** Changes to atmospheric temperature and chemical composition as functions of latitude and altitude for MAM-60 (left) and ANN-60 (right), relative to RCP8.5 during the same period (2035-2039). Figures 4a and 4b (top) plot changes to SO<sub>4</sub> mixing ratio, Figures 4c and 4d (middle) plot temperature change, and Figures 4e and 4f (bottom) plot changes to ozone concentration. All changes are averaged over the last five years of simulation and normalized by the average extent of SSI restored relative to RCP8.5.

232 in the upper troposphere-lowermost stratosphere near the equator, and further strato-  
233 spheric ozone destruction over the Arctic compared with MAM-60.

234 One of the expected changes from focusing a geoengineered cooling over the Arctic  
235 would be an increase in meridional heat transport (Tilmes et al., 2014), and conse-  
236 quent shifts in tropical precipitation (Robock et al., 2008; MacCracken et al., 2013; Kravitz  
237 et al., 2016). Changes to meridional heat transport at 60°N are small for both MAM-  
238 60 and ANN-60. The total meridional heat flux at 60°N under RCP8.5 in the years 2035-  
239 2039 (computed by the top-of-atmosphere radiation balance as in Wunsch (2005)) is  $3.41$   
240  $\pm 0.01$  PW; ANN-60 shows no statistically detectable change, while MAM-60 shows a  
241 slight increase to  $3.45 \pm 0.01$  PW. Both MAM-60 and ANN-60 show detectable changes  
242 to tropical heat transport. We define the ITCZ as the latitude of zero meridional heat  
243 transport, as in Byrne et al. (2018); by fitting a linear function to meridional heat trans-  
244 port as a function of latitude between 10°S and 10°N and solving for the intercept, we  
245 compute an ITCZ located at  $-2.4 \pm 0.1$  degrees latitude for RCP8.5. ANN-60 pushes the  
246 ITCZ south to  $-2.9 \pm 0.1$  degrees, and MAM-60 shifts the ITCZ further to  $-3.4 \pm 0.1$   
247 degrees, approximately a factor of two; this is consistent with the understanding that  
248 SAI in one hemisphere pushes the ITCZ towards the other hemisphere (Haywood et al.,  
249 2013). This change in ITCZ likely impacts tropical precipitation, but computing the trop-  
250 ical precipitation centroid from 20°S to 20°N as in Lee et al 2020 shows no statistically  
251 significant change from RCP8.5. Comparisons of SSI extent, temperature, heat trans-  
252 port, and tropical precipitation values for RCP8.5, MAM-60, and ANN-60 can be found  
253 in the supplementary material.

## 254 4 Discussion and Conclusions

255 In this study, we directly compare simulations of year-round and spring SAI in the  
256 Arctic. Per teragram of SO<sub>2</sub> injected, spring injection at 60°N restores approximately  
257 twice as much SSI and achieves approximately 1.5 times the Arctic and global mean tem-  
258 perature reductions as year-round injection. Assuming that the climate responds approx-  
259 imately linearly to small changes in radiative forcing, spring injection could achieve sim-  
260 ilar climate goals to year-round injection with one-half to two-thirds the injection quan-  
261 tity, resulting in smaller increases to stratospheric sulfur burden, stratospheric heating,  
262 and stratospheric ozone depletion, as well as less surface acid rain deposition (Visioni,  
263 Slessarev, et al., 2020).

264 The primary focus of this study is the efficacy of seasonal versus year-round SAI  
265 in preserving SSI; we only look at a few of the relevant impacts, and we do so in only  
266 one climate model. In order to support informed future decisions around SAI in general  
267 and Arctic-focused SAI in particular, a much more careful evaluation of multiple differ-  
268 ent climate impacts would be necessary, especially considering the interconnectedness  
269 of the Arctic climate: Greenland ice sheet melt is strongly influenced by any changes in  
270 cloud cover (Hofer et al., 2017), permafrost thaw is affected by changes in snow depth  
271 that provide insulation, etc. A model intercomparison would also be critical to under-  
272 stand confidence. Furthermore, while it is clear from our results that the biggest impact  
273 on efficiency arises from focusing injection in the spring, there is more work that needs  
274 to be done to better understand trade-offs with injection altitude, latitude, and timing.  
275 The different AOD seasonal cycles of MAM-60, AM-60, and AMJ-60 demonstrate that  
276 we can change the timing of the AOD peak; while the peak AOD of MAM-60 coincides  
277 with peak insolation in June, there is more reflective sea ice then than there is later in  
278 the year, and so the detailed relationship between the injection timing or duration and  
279 sea ice recovery is not obvious and likely depends on the extent of summer sea ice re-  
280 maining in a given year. Additionally, depending on the objectives of a hypothetical fu-  
281 ture geoengineering deployment, it may be useful to consider injecting at multiple dif-  
282 ferent latitudes simultaneously to manage different goals. For example, SAI in one hemi-  
283 sphere pushes the ITCZ towards the other hemisphere (Sun et al., 2020), so another in-

284 jection at 60°S or other latitudes in the Southern Hemisphere could counteract the ef-  
 285 fects of Arctic SAI on low-latitude heat transport as proposed by MacCracken et al (2014)  
 286 and Kravitz et al. (2016). Finally, we note that in contrast to more “globally” focused  
 287 strategies that have been the focus of almost all modeling work, as well as the context  
 288 motivating most governance studies, Arctic-focused SAI could be deployed without the  
 289 development of new aircraft capability. Combined with potential concerns over climate  
 290 change in the Arctic, it is plausible that Arctic-focused SAI may be more likely to be  
 291 deployed, and sooner, than any global SAI strategy.

## 292 Acknowledgments

293 We would like to acknowledge high-performance computing support from Cheyenne (doi:10.5065/D6RX99HX)  
 294 provided by NCAR’s Computational and Information Systems Laboratory, sponsored  
 295 by the National Science Foundation. Support for WL and DM was provided by the Na-  
 296 tional Science Foundation through agreement CBET-1818759. Support for DV was pro-  
 297 vided by the Atkinson Center for a Sustainable Future at Cornell University. Support  
 298 for BK was provided in part by the National Sciences Foundation through agreement  
 299 CBET-1931641, the Indiana University Environmental Resilience Institute, and the *Pre-*  
 300 *pared for Environmental Change* Grand Challenge initiative. The Pacific Northwest Na-  
 301 tional Laboratory is operated for the U.S. Department of Energy by Battelle Memorial  
 302 Institute under contract DE-AC05-76RL01830. The CESM project is supported primar-  
 303 ily by the National Science Foundation. This work was supported by the National Cen-  
 304 ter for Atmospheric Research, which is a major facility sponsored by the National Sci-  
 305 ence Foundation under Cooperative Agreement No. 1852977. Data will be made avail-  
 306 able online through the Cornell e-Commons Library.

## 307 References

- 308 Ballinger, T. J., Overland, J. E., Wang, M., Bhatt, U. S., Hanna, E., Hanssen-  
 309 Bauer, I., ... Walsh, J. E. (2020). *Arctic report card 2020: Surface air tem-*  
 310 *perature*. Retrieved from [https://www.arctic.noaa.gov/Report-Card/](https://www.arctic.noaa.gov/Report-Card/Report-Card-2020/ArtMID/7975/ArticleID/878/Surface-Air-Temperature)  
 311 [Report-Card-2020/ArtMID/7975/ArticleID/878/Surface-Air-Temperature](https://www.arctic.noaa.gov/Report-Card-2020/ArtMID/7975/ArticleID/878/Surface-Air-Temperature)  
 312 doi: DOI:10.25923/gcw8-2z06
- 313 Barber, D. G., Meier, W. N., Gerland, S., Mundy, C., Holland, M., Kern, S., ...  
 314 Tamura, T. (2017). *Snow, water, ice and permafrost in the arctic (swipa)*  
 315 *2017: Arctic sea ice*. Retrieved from [https://www.amap.no/documents/](https://www.amap.no/documents/download/2987/inline)  
 316 [download/2987/inline](https://www.amap.no/documents/download/2987/inline)
- 317 Byrne, M. P., Pendergrass, A. G., Rapp, A. D., & Wodzicki, K. R. (2018). Response  
 318 of the intertropical convergence zone to climate change: Location, width, and  
 319 strength. *Current Climate Change Reports*, 4, 355–370. Retrieved from  
 320 <https://link.springer.com/article/10.1007/s40641-018-0110-5> doi:  
 321 <https://doi.org/10.1007/s40641-018-0110-5>
- 322 Caldeira, K., & Wood, L. (2008). Global and arctic climate engineering: numerical  
 323 model studies. *Philosophical Transactions of the Royal Society A: Mathemati-*  
 324 *cal, Physical and Engineering Sciences*, 366(1882), 4039-4056. Retrieved from  
 325 <https://royalsocietypublishing.org/doi/abs/10.1098/rsta.2008.0132>  
 326 doi: 10.1098/rsta.2008.0132
- 327 Chen, Y., Liu, A., & Moore, J. C. (2020). Mitigation of arctic permafrost car-  
 328 bon loss through stratospheric aerosol geoengineering. *Nature Communi-*  
 329 *cations*, 11(2430). Retrieved from [https://www.nature.com/articles/](https://www.nature.com/articles/s41467-020-16357-8)  
 330 [s41467-020-16357-8](https://www.nature.com/articles/s41467-020-16357-8) doi: <https://doi.org/10.1038/s41467-020-16357-8>
- 331 Cice: the los alamos sea ice model documentation and software user’s manual [Com-  
 332 puter software manual]. (2010). Los Alamos NM 87545. Retrieved from  
 333 [https://csdms.colorado.edu/w/images/CICE\\_documentation\\_and\\_software](https://csdms.colorado.edu/w/images/CICE_documentation_and_software_user%27s_manual.pdf)  
 334 [\\_user%27s\\_manual.pdf](https://csdms.colorado.edu/w/images/CICE_documentation_and_software_user%27s_manual.pdf)

- 335 Dai, Z., Weisenstein, D. K., & Keith, D. W. (2018). Tailoring meridional and  
 336 seasonal radiative forcing by sulfate aerosol solar geoengineering. *Geo-*  
 337 *physical Research Letters*, *45*(2), 1030-1039. Retrieved from [https://](https://agupubs.onlinelibrary.wiley.com/doi/abs/10.1002/2017GL076472)  
 338 [agupubs.onlinelibrary.wiley.com/doi/abs/10.1002/2017GL076472](https://agupubs.onlinelibrary.wiley.com/doi/abs/10.1002/2017GL076472) doi:  
 339 10.1002/2017GL076472
- 340 DuVivier, A. K., DeRepentigny, P., Holland, M. M., Webster, M., Kay, J. E., & Per-  
 341 ovich, D. (2020). Going with the floe: tracking cesm large ensemble sea ice in  
 342 the arctic provides context for ship-based observations. *The Cryosphere*, *14*(4),  
 343 1259–1271. Retrieved from [https://tc.copernicus.org/articles/14/1259/](https://tc.copernicus.org/articles/14/1259/2020/)  
 344 [2020/](https://tc.copernicus.org/articles/14/1259/2020/) doi: 10.5194/tc-14-1259-2020
- 345 Ferraro, A. J., Charlton-Perez, A. J., & Highwood, E. J. (2015). Stratospheric  
 346 dynamics and midlatitude jets under geoengineering with space mirrors  
 347 and sulfate and titania aerosols. *Journal of Geophysical Research: Atmo-*  
 348 *spheres*, *120*(2), 414-429. Retrieved from [https://agupubs.onlinelibrary](https://agupubs.onlinelibrary.wiley.com/doi/abs/10.1002/2014JD022734)  
 349 [.wiley.com/doi/abs/10.1002/2014JD022734](https://agupubs.onlinelibrary.wiley.com/doi/abs/10.1002/2014JD022734) doi: [https://doi.org/10.1002/](https://doi.org/10.1002/2014JD022734)  
 350 [2014JD022734](https://doi.org/10.1002/2014JD022734)
- 351 Fyfe, J. C., von Salzen, K., Gillett, N. P., Arora, V. K., Flato, G. M., & Mc-  
 352 Connell, J. R. (2013). One hundred years of arctic surface temperature  
 353 variation due to anthropogenic influence. *Scientific Reports*, *3*(2645).  
 354 Retrieved from <https://www.nature.com/articles/srep02645> doi:  
 355 <https://doi.org/10.1038/srep02645>
- 356 Haine, T. W. N., & Martin, T. (2017). The arctic-subarctic sea ice system is enter-  
 357 ing a seasonal regime: Implications for future arctic amplification. *Scientific*  
 358 *Reports*, *7*(4618). Retrieved from [https://www.nature.com/articles/](https://www.nature.com/articles/s41598-017-04573-0)  
 359 [s41598-017-04573-0](https://www.nature.com/articles/s41598-017-04573-0) doi: <https://doi.org/10.1038/s41598-017-04573-0>
- 360 Harari, O., Garfinkel, C. I., Ziskin Ziv, S., Morgenstern, O., Zeng, G., Tilmes, S., ...  
 361 Davis, S. (2019). Influence of arctic stratospheric ozone on surface climate in  
 362 ccmi models. *Atmospheric Chemistry and Physics*, *19*(14), 9253–9268. Re-  
 363 trieved from <https://acp.copernicus.org/articles/19/9253/2019/> doi:  
 364 10.5194/acp-19-9253-2019
- 365 Haywood, J. M., Jones, A., Bellouin, N., & Stephenson, D. (2013). Asymmet-  
 366 ric forcing from stratospheric aerosols impacts Sahelian rainfall. *Nature*  
 367 *Climate Change*, *3*, 660–665. Retrieved from [https://doi.org/10.1038/](https://doi.org/10.1038/nclimate1857)  
 368 [nclimate1857](https://doi.org/10.1038/nclimate1857) (doi:10.1038/nclimate1857) doi: 10.1038/nclimate1857
- 369 Hofer, S., Tedstone, A. J., Fettweis, X., & Bamber, J. L. (2017). Decreasing cloud  
 370 cover drives the recent mass loss on the greenland ice sheet. *Science Advances*,  
 371 *3*(6). Retrieved from [https://advances.sciencemag.org/content/3/6/](https://advances.sciencemag.org/content/3/6/e1700584)  
 372 [e1700584](https://advances.sciencemag.org/content/3/6/e1700584) doi: 10.1126/sciadv.1700584
- 373 Jackson, L. S., Crook, J. A., Jarvis, A., Leedal, D., Ridgwell, A., Vaughan, N., &  
 374 Forster, P. M. (2015). Assessing the controllability of arctic sea ice extent  
 375 by sulfate aerosol geoengineering. *Geophysical Research Letters*, *42*(4), 1223-  
 376 1231. Retrieved from [https://agupubs.onlinelibrary.wiley.com/doi/abs/](https://agupubs.onlinelibrary.wiley.com/doi/abs/10.1002/2014GL062240)  
 377 [10.1002/2014GL062240](https://agupubs.onlinelibrary.wiley.com/doi/abs/10.1002/2014GL062240) doi: 10.1002/2014GL062240
- 378 Jiang, J., Cao, L., MacMartin, D. G., Simpson, I. R., Kravitz, B., Cheng, W., ...  
 379 Mills, M. J. (2019). Stratospheric sulfate aerosol geoengineering could alter  
 380 the high-latitude seasonal cycle. *Geophysical Research Letters*, *46*(23), 14153-  
 381 14163. Retrieved from [https://agupubs.onlinelibrary.wiley.com/doi/](https://agupubs.onlinelibrary.wiley.com/doi/abs/10.1029/2019GL085758)  
 382 [abs/10.1029/2019GL085758](https://agupubs.onlinelibrary.wiley.com/doi/abs/10.1029/2019GL085758) doi: 10.1029/2019GL085758
- 383 Kay, J. E., Holland, M. M., & Jahn, A. (2011). Inter-annual to multi-decadal arctic  
 384 sea ice extent trends in a warming world. *Geophysical Research Letters*,  
 385 *38*(15). Retrieved from [https://agupubs.onlinelibrary.wiley.com/doi/](https://agupubs.onlinelibrary.wiley.com/doi/abs/10.1029/2011GL048008)  
 386 [abs/10.1029/2011GL048008](https://agupubs.onlinelibrary.wiley.com/doi/abs/10.1029/2011GL048008) doi: <https://doi.org/10.1029/2011GL048008>
- 387 Kravitz, B., Macmartin, D., Wang, H., & Rasch, P. (2016, 05). Geoengineering as a  
 388 design problem. *Earth System Dynamics*, *7*, 469-497. doi: 10.5194/esd-7-469-  
 389 -2016

- 390 Kravitz, B., MacMartin, D. G., Mills, M. J., Richter, J. H., Tilmes, S., Lamar-  
 391 que, J.-F., ... Vitt, F. (2017). First simulations of designing stratospheric  
 392 sulfate aerosol geoengineering to meet multiple simultaneous climate objec-  
 393 tives. *Journal of Geophysical Research: Atmospheres*, *122*(23), 12,616-12,634.  
 394 Retrieved from [https://agupubs.onlinelibrary.wiley.com/doi/abs/](https://agupubs.onlinelibrary.wiley.com/doi/abs/10.1002/2017JD026874)  
 395 [10.1002/2017JD026874](https://doi.org/10.1002/2017JD026874) doi: 10.1002/2017JD026874
- 396 Kravitz, B., Robock, A., Boucher, O., Schmidt, H., Taylor, K. E., Stenchikov, G.,  
 397 & Schulz, M. (2011). The geoengineering model intercomparison project  
 398 (geomip). *Atmospheric Science Letters*, *12*(2), 162-167. Retrieved from  
 399 <https://rmets.onlinelibrary.wiley.com/doi/abs/10.1002/asl.316> doi:  
 400 <https://doi.org/10.1002/asl.316>
- 401 Lee, W., MacMartin, D., Vioni, D., & Kravitz, B. (2020). Expanding the design  
 402 space of stratospheric aerosol geoengineering to include precipitation-based  
 403 objectives and explore trade-offs. *Earth System Dynamics*, *11*(4), 1051–1072.  
 404 Retrieved from <https://esd.copernicus.org/articles/11/1051/2020/>  
 405 doi: 10.5194/esd-11-1051-2020
- 406 Liu, X., Easter, R. C., Ghan, S. J., Zaveri, R., Rasch, P., Shi, X., ... Mitchell,  
 407 D. (2012). Toward a minimal representation of aerosols in climate mod-  
 408 els: description and evaluation in the community atmosphere model cam5.  
 409 *Geoscientific Model Development*, *5*(3), 709–739. Retrieved from [https://](https://gmd.copernicus.org/articles/5/709/2012/)  
 410 [gmd.copernicus.org/articles/5/709/2012/](https://gmd.copernicus.org/articles/5/709/2012/) doi: 10.5194/gmd-5-709-2012
- 411 MacCracken, M., Shin, H.-J., Caldeira, K., & Ban-Weiss, G. (2013, 09). Climate  
 412 response to imposed solar radiation reductions in high latitudes. *Earth System*  
 413 *Dynamics*, *4*. doi: 10.5194/esd-4-301-2013
- 414 Meredith, M., Sommerkorn, M., Cassotta, S., Derksen, C., Ekaykin, A., Hollowed,  
 415 A., ... Schuur, E. (2019). *Ipc special report on the ocean and cryosphere in*  
 416 *a changing climate: Polar regions* (H.-O. Pörtner et al., Eds.). Retrieved from  
 417 <https://www.ipcc.ch/srocc/>
- 418 Mills, M. J., Richter, J. H., Tilmes, S., Kravitz, B., MacMartin, D. G., Glanville,  
 419 A. A., ... Kinnison, D. E. (2017). Radiative and chemical response to inter-  
 420 active stratospheric sulfate aerosols in fully coupled cesm1(waccm). *Journal*  
 421 *of Geophysical Research: Atmospheres*, *122*(23), 13,061-13,078. Retrieved  
 422 from [https://agupubs.onlinelibrary.wiley.com/doi/abs/10.1002/](https://agupubs.onlinelibrary.wiley.com/doi/abs/10.1002/2017JD027006)  
 423 [2017JD027006](https://doi.org/10.1002/2017JD027006) doi: 10.1002/2017JD027006
- 424 Mills, M. J., Schmidt, A., Easter, R., Solomon, S., Kinnison, D. E., Ghan, S. J.,  
 425 ... Gettelman, A. (2016). Global volcanic aerosol properties derived  
 426 from emissions, 1990–2014, using cesm1(waccm). *Journal of Geophys-ical*  
 427 *Research: Atmospheres*, *121*(5), 2332-2348. Retrieved from [https://](https://agupubs.onlinelibrary.wiley.com/doi/abs/10.1002/2015JD024290)  
 428 [agupubs.onlinelibrary.wiley.com/doi/abs/10.1002/2015JD024290](https://agupubs.onlinelibrary.wiley.com/doi/abs/10.1002/2015JD024290) doi:  
 429 [10.1002/2015JD024290](https://doi.org/10.1002/2015JD024290)
- 430 Moore, J. C., Yue, C., Zhao, L., Guo, X., Watanabe, S., & Ji, D. (2019).  
 431 Greenland ice sheet response to stratospheric aerosol injection geoen-  
 432 gineering. *Earth's Future*, *7*(12), 1451-1463. Retrieved from [https://](https://agupubs.onlinelibrary.wiley.com/doi/abs/10.1029/2019EF001393)  
 433 [agupubs.onlinelibrary.wiley.com/doi/abs/10.1029/2019EF001393](https://agupubs.onlinelibrary.wiley.com/doi/abs/10.1029/2019EF001393) doi:  
 434 <https://doi.org/10.1029/2019EF001393>
- 435 Notz, D., & Marotzke, J. (2012). Observations reveal external driver for arctic sea-  
 436 ice retreat. *Geophysical Research Letters*, *39*(8). Retrieved from [https://](https://agupubs.onlinelibrary.wiley.com/doi/abs/10.1029/2012GL051094)  
 437 [agupubs.onlinelibrary.wiley.com/doi/abs/10.1029/2012GL051094](https://agupubs.onlinelibrary.wiley.com/doi/abs/10.1029/2012GL051094) doi:  
 438 <https://doi.org/10.1029/2012GL051094>
- 439 Notz, D., & Stroeve, J. (2016). Observed arctic sea-ice loss directly follows  
 440 anthropogenic co2 emission. *Science*, *354*(6313), 747–750. Retrieved  
 441 from <https://science.sciencemag.org/content/354/6313/747> doi:  
 442 [10.1126/science.aag2345](https://doi.org/10.1126/science.aag2345)
- 443 Peixoto, J. P., & Oort, A. H. (1992). *Physics of climate* (1st ed.). AIP-Press.

- 444 Peng, G., Steele, M., Bliss, A. C., Meier, W. N., & Dickinson, S. (2018). Temporal  
 445 means and variability of arctic sea ice melt and freeze season climate indicators  
 446 using a satellite climate data record. *Remote Sensing*, *10*(9). Retrieved from  
 447 <https://www.mdpi.com/2072-4292/10/9/1328> doi: 10.3390/rs10091328
- 448 Perovich, D., Meier, W., Tschudi, M., Hendricks, S., Petty, A. A., Divine, D.,  
 449 ... Wood, K. (2020). *Arctic report card 2020: Sea ice*. Retrieved from  
 450 [https://arctic.noaa.gov/Report-Card/Report-Card-2020/ArtMID/7975/](https://arctic.noaa.gov/Report-Card/Report-Card-2020/ArtMID/7975/ArticleID/891/Sea-Ice)  
 451 [ArticleID/891/Sea-Ice](https://arctic.noaa.gov/Report-Card/Report-Card-2020/ArtMID/7975/ArticleID/891/Sea-Ice) doi: 10.25923/n170-9h57
- 452 Perovich, D. K., & Polashenski, C. (2012). Albedo evolution of seasonal arctic sea  
 453 ice. *Geophysical Research Letters*, *39*(8). Retrieved from [https://agupubs](https://agupubs.onlinelibrary.wiley.com/doi/abs/10.1029/2012GL051432)  
 454 [.onlinelibrary.wiley.com/doi/abs/10.1029/2012GL051432](https://agupubs.onlinelibrary.wiley.com/doi/abs/10.1029/2012GL051432) doi: [https://](https://doi.org/10.1029/2012GL051432)  
 455 [doi.org/10.1029/2012GL051432](https://doi.org/10.1029/2012GL051432)
- 456 Pistone, K., Eisenman, I., & Ramanathan, V. (2014). Observational determination  
 457 of albedo decrease caused by vanishing arctic sea ice. *Proceedings of the Na-*  
 458 *tional Academy of Sciences*, *111*(9), 3322–3326. Retrieved from [https://www](https://www.pnas.org/content/111/9/3322)  
 459 [.pnas.org/content/111/9/3322](https://www.pnas.org/content/111/9/3322) doi: 10.1073/pnas.1318201111
- 460 Pithan, F., & Mauritsen, T. (2014). Arctic amplification dominated by temper-  
 461 ature feedbacks in contemporary climate models. *Nature Geoscience*, *7*, 181–  
 462 184. Retrieved from <https://www.nature.com/articles/ngeo2071> doi:  
 463 <https://doi.org/10.1038/ngeo2071>
- 464 Roberts, A. F., Hunke, E. C., Allard, R., Bailey, D. A., Craig, A. P., Lemieux, J.-F.,  
 465 & Turner, M. D. (2018). Quality control for community-based sea-ice model  
 466 development. *Philosophical Transactions of the Royal Society A: Mathematical,*  
 467 *Physical and Engineering Sciences*, *376*(2129), 20170344. Retrieved from  
 468 <https://royalsocietypublishing.org/doi/abs/10.1098/rsta.2017.0344>  
 469 doi: 10.1098/rsta.2017.0344
- 470 Robock, A., Oman, L., & Stenchikov, G. L. (2008). Regional climate responses  
 471 to geoengineering with tropical and arctic so<sub>2</sub> injections. *Journal of Geo-*  
 472 *physical Research: Atmospheres*, *113*(D16). Retrieved from [https://](https://agupubs.onlinelibrary.wiley.com/doi/abs/10.1029/2008JD010050)  
 473 [agupubs.onlinelibrary.wiley.com/doi/abs/10.1029/2008JD010050](https://agupubs.onlinelibrary.wiley.com/doi/abs/10.1029/2008JD010050) doi:  
 474 [10.1029/2008JD010050](https://doi.org/10.1029/2008JD010050)
- 475 Robrecht, S., Vogel, B., Tilmes, S., & Müller, R. (2020). Potential of future strato-  
 476 spheric ozone loss in the mid-latitudes under climate change and sulfate geo-  
 477 engineering. *Atmospheric Chemistry and Physics Discussions*, *2020*, 1–40.  
 478 Retrieved from <https://acp.copernicus.org/preprints/acp-2020-747/>  
 479 doi: 10.5194/acp-2020-747
- 480 Rogelj, J., den Elzen, M., Höhne, N., Fransen, T., Fekete, H., Winkler, H., ...  
 481 Meinshausen, M. (2016). Paris agreement climate proposals need a boost  
 482 to keep warming well below 2°C. *Nature*, *534*, 631–639. Retrieved from  
 483 <https://www.nature.com/articles/nature18307> doi: [https://doi.org/](https://doi.org/10.1038/nature18307)  
 484 [10.1038/nature18307](https://doi.org/10.1038/nature18307)
- 485 Snape, T. J., & Forster, P. M. (2014). Decline of arctic sea ice: Evaluation and  
 486 weighting of cmip5 projections. *Journal of Geophysical Research: Atmo-*  
 487 *spheres*, *119*(2), 546–554. Retrieved from [https://agupubs.onlinelibrary](https://agupubs.onlinelibrary.wiley.com/doi/abs/10.1002/2013JD020593)  
 488 [.wiley.com/doi/abs/10.1002/2013JD020593](https://agupubs.onlinelibrary.wiley.com/doi/abs/10.1002/2013JD020593) doi: [https://doi.org/10.1002/](https://doi.org/10.1002/2013JD020593)  
 489 [2013JD020593](https://doi.org/10.1002/2013JD020593)
- 490 Stroeve, J., & Notz, D. (2018, sep). Changing state of arctic sea ice across all  
 491 seasons. *Environmental Research Letters*, *13*(10), 103001. Retrieved from  
 492 <https://doi.org/10.1088/1748-9326/aade56> doi: 10.1088/1748-9326/  
 493 [aade56](https://doi.org/10.1088/1748-9326/aade56)
- 494 Stroeve, J. C., Serreze, M. C., Holland, M. M., Kay, J. E., Malanik, J., & Bar-  
 495 rett, A. P. (2012). The arctic's rapidly shrinking sea ice cover: a re-  
 496 search synthesis. *Climatic Change*, *110*, 1005–1027. Retrieved from  
 497 <https://link.springer.com/article/10.1007/s10584-011-0101-1> doi:  
 498 <https://doi.org/10.1007/s10584-011-0101-1>

- 499 Sun, W., Wang, B., Chen, D., Gao, C., Lu, G., & Liu, J. (2020). Global monsoon  
500 response to tropical and arctic stratospheric aerosol injection. *Climate Dynam-*  
501 *ics*, *55*, 2107–2121. Retrieved from [https://link.springer.com/article/](https://link.springer.com/article/10.1007/s00382-020-05371-7)  
502 [10.1007/s00382-020-05371-7](https://link.springer.com/article/10.1007/s00382-020-05371-7) doi: [https://doi.org/10.1007/s00382-020-05371-](https://doi.org/10.1007/s00382-020-05371-7)  
503 [-7](https://doi.org/10.1007/s00382-020-05371-7)
- 504 Tilmes, S., Jahn, A., Kay, J. E., Holland, M., & Lamarque, J.-F. (2014). Can  
505 regional climate engineering save the summer arctic sea ice? *Geophys-*  
506 *ical Research Letters*, *41*(3), 880-885. Retrieved from [https://agupubs](https://agupubs.onlinelibrary.wiley.com/doi/abs/10.1002/2013GL058731)  
507 [.onlinelibrary.wiley.com/doi/abs/10.1002/2013GL058731](https://agupubs.onlinelibrary.wiley.com/doi/abs/10.1002/2013GL058731) doi:  
508 <https://doi.org/10.1002/2013GL058731>
- 509 Tilmes, S., Richter, J. H., Kravitz, B., MacMartin, D. G., Mills, M. J., Simpson,  
510 I. R., ... Ghosh, S. (2018, 12). CESM1(WACCM) Stratospheric Aerosol  
511 Geoengineering Large Ensemble Project. *Bulletin of the American Meteorolog-*  
512 *ical Society*, *99*(11), 2361-2371. Retrieved from [https://doi.org/10.1175/](https://doi.org/10.1175/BAMS-D-17-0267.1)  
513 [BAMS-D-17-0267.1](https://doi.org/10.1175/BAMS-D-17-0267.1) doi: [10.1175/BAMS-D-17-0267.1](https://doi.org/10.1175/BAMS-D-17-0267.1)
- 514 Visioni, D., MacMartin, D. G., & Kravitz, B. (2020). Is turning down the sun  
515 a good proxy for stratospheric sulfate geoengineering? *Earth and Space*  
516 *Science Open Archive*, *50*. Retrieved from [https://doi.org/10.1002/](https://doi.org/10.1002/essoar.10504448.1)  
517 [essoar.10504448.1](https://doi.org/10.1002/essoar.10504448.1) doi: [10.1002/essoar.10504448.1](https://doi.org/10.1002/essoar.10504448.1)
- 518 Visioni, D., MacMartin, D. G., Kravitz, B., Lee, W., Simpson, I. R., & Richter,  
519 J. H. (2020). Reduced poleward transport due to stratospheric heating  
520 under stratospheric aerosols geoengineering. *Geophysical Research Letters*,  
521 *47*(17), e2020GL089470. Retrieved from [https://agupubs.onlinelibrary](https://agupubs.onlinelibrary.wiley.com/doi/abs/10.1029/2020GL089470)  
522 [.wiley.com/doi/abs/10.1029/2020GL089470](https://agupubs.onlinelibrary.wiley.com/doi/abs/10.1029/2020GL089470) (e2020GL089470  
523 [10.1029/2020GL089470](https://doi.org/10.1029/2020GL089470)) doi: [10.1029/2020GL089470](https://doi.org/10.1029/2020GL089470)
- 524 Visioni, D., MacMartin, D. G., Kravitz, B., Richter, J. H., Tilmes, S., & Mills, M. J.  
525 (2020). Seasonally modulated stratospheric aerosol geoengineering alters the  
526 climate outcomes. *Geophysical Research Letters*, *47*(12), e2020GL088337.  
527 Retrieved from [https://agupubs.onlinelibrary.wiley.com/doi/abs/](https://agupubs.onlinelibrary.wiley.com/doi/abs/10.1029/2020GL088337)  
528 [10.1029/2020GL088337](https://agupubs.onlinelibrary.wiley.com/doi/abs/10.1029/2020GL088337) (e2020GL088337 2020GL088337) doi: [10.1029/](https://doi.org/10.1029/2020GL088337)  
529 [2020GL088337](https://doi.org/10.1029/2020GL088337)
- 530 Visioni, D., Slessarev, E., MacMartin, D. G., Mahowald, N. M., Goodale, C. L., &  
531 Xia, L. (2020, sep). What goes up must come down: impacts of deposition  
532 in a sulfate geoengineering scenario. *Environmental Research Letters*, *15*(9),  
533 094063. Retrieved from <https://doi.org/10.1088/1748-9326/ab94eb> doi:  
534 [10.1088/1748-9326/ab94eb](https://doi.org/10.1088/1748-9326/ab94eb)
- 535 WANG, H., ZHANG, L., CHU, M., & HU, S. (2020). Advantages of the latest  
536 los alamos sea-ice model (cice): evaluation of the simulated spatiotemporal  
537 variation of arctic sea ice. *Atmospheric and Oceanic Science Letters*, *13*(2),  
538 113-120. Retrieved from <https://doi.org/10.1080/16742834.2020.1712186>  
539 doi: [10.1080/16742834.2020.1712186](https://doi.org/10.1080/16742834.2020.1712186)
- 540 Wunsch, C. (2005). The total meridional heat flux and its oceanic and atmospheric  
541 partition. *Journal of Climate*, *18*(21), 4374 - 4380. Retrieved from [https://](https://journals.ametsoc.org/view/journals/clim/18/21/jcli3539.1.xml)  
542 [journals.ametsoc.org/view/journals/clim/18/21/jcli3539.1.xml](https://journals.ametsoc.org/view/journals/clim/18/21/jcli3539.1.xml) doi:  
543 [10.1175/JCLI3539.1](https://doi.org/10.1175/JCLI3539.1)
- 544 Årthun, M., Onarheim, I. H., Dörr, J., & Eldevik, T. (2021). The seasonal and  
545 regional transition to an ice-free arctic. *Geophysical Research Letters*, *48*(1),  
546 e2020GL090825. Retrieved from [https://agupubs.onlinelibrary.wiley](https://agupubs.onlinelibrary.wiley.com/doi/abs/10.1029/2020GL090825)  
547 [.com/doi/abs/10.1029/2020GL090825](https://agupubs.onlinelibrary.wiley.com/doi/abs/10.1029/2020GL090825) (e2020GL090825 2020GL090825) doi:  
548 <https://doi.org/10.1029/2020GL090825>